Article

C-mannosyl lysine for solid phase assembly of mannosylated peptide conjugate cancer vaccines

Tim P. Hogervorst, R.J. Eveline Li, Laura Marino, Sven C.M. Bruijns, Nico J. Meeuwenoord, Dmitri V. Filippov, Herman S. Overkleeft, Gijsbert A. van der Marel, Sandra J. van Vliet, Yvette van Kooyk, and Jeroen D. C. Codée

ACS Chem. Biol., **Just Accepted Manuscript** • DOI: 10.1021/acschembio.9b00987 • Publication Date (Web): 11 Feb 2020

C-mannosyl lysine for solid phase assembly of mannosylated peptide conjugate cancer vaccines

Tim P. Hogervorst[1]†, R.J. Eveline Li[2]†, Laura Marino[1], Sven C.M. Bruijns[2], Nico J. Meeuwenoord[1], Dmitri V. Filippov[1], Herman S. Overkleeft[1], Gijsbert A. van der Marel[1], Sandra J. van Vliet[2], Yvette van Kooyk[2]* and Jeroen D.C. Codée[1]*

[1] Department of Bio-organic Synthesis, Faculty of Science, Leiden Institute of Chemistry, Leiden University, Leiden, The Netherlands, [2] Amsterdam UMC- location Vrije Universiteit Amsterdam, dept. of Molecular Cell Biology and Immunology, Cancer Center Amsterdam, Amsterdam Infection and Immunity Institute, Amsterdam, Netherlands

† These authors have contributed equally to this work

* Correspondence:
Jeroen D.C. Codée
JCodee@chem.leidenuniv.nl

Yvette van Kooyk
Y.vanKooyk@amsterdamumc.nl

Graphical Abstract

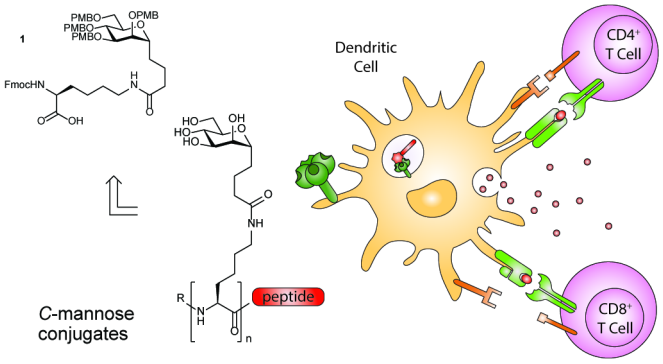

Abstract

Dendritic cells (DCs) are armed with a multitude of Pattern Recognition Receptors (PRRs) to recognize pathogens and initiate pathogen-tailored T cell responses. In these responses, the maturation of DCs is key, as well as the production of cytokines that help to accomplish T cell responses. DC-SIGN is a frequently exploited PRR that can effectively be targeted with mannosylated antigens to enhance the induction of antigen-specific T cells. The natural *O*-mannosidic linkage is susceptible to enzymatic degradation, and its chemical sensitivity complicates the synthesis of mannosylated antigens. For this reason, (oligo)mannosides are generally introduced in a late stage of the antigen synthesis, requiring orthogonal conjugation handles for their attachment. To increase the stability of the mannosides and streamline the synthesis of mannosylated peptide antigens, we here describe the development of an acid-stable *C*-mannosyl lysine, which allows for the inline introduction of mannosides during solid-phase peptide synthesis (SPPS). The developed amino acid has been successfully used for the assembly of both small ligands and peptide antigen conjugates comprising an epitope of the gp100 melanoma-associated antigen and a TLR7 agonist for DC activation. The ligands showed similar internalization capacities and binding affinities as the *O*-mannosyl analogs. Moreover, the antigen conjugates were capable of inducing maturation, stimulating the secretion of pro-inflammatory cytokines, and providing enhanced gp100 presentation to $CD8^+$ and $CD4^+$ T cells, similar to their *O*-mannosyl counterparts. Our results demonstrate that the *C*-mannose lysine is a valuable building block for the generation of anti-cancer peptide-conjugate vaccine modalities.

Keywords: glycopeptides, *C*-glycoside, peptide conjugate, vaccine model, DC-SIGN

INTRODUCTION

Immunotherapy for cancer is gaining momentum. More and more therapies have reached the clinic or are in advanced clinical trials, including immune checkpoint blocking (ICB) antibodies, chimeric antigen receptor T cells (CAR T cells), adoptive cell transfer (ACT), and dendritic cell (DC) vaccination.[1–4] DC-based strategies rely on the role of dendritic cells as key initiators of the adaptive immune system that are crucial in the induction of memory responses. By antigen capture and processing, DCs can present peptides to naïve T lymphocytes and skew their differentiation endpoints and by exposing DCs to synthetic tumor (neo-)antigens, the immune response can be directed towards specific cancer-associated antigens. Although animal models have demonstrated promising results for peptide-based vaccine strategies, human trials often result in minimal tumor regression and only partial effectiveness[5,6]. Vaccine efficacy may be improved by the incorporation of adjuvants that can target Pattern Recognition Receptors (PRRs), which can induce DC maturation and improve antigen processing[7]. Toll-Like Receptors (TLRs) are a family of PRRs, of which members have been successfully targeted with covalent adjuvant-antigen conjugates[8–12], to induce DC maturation and improve antigen processing and presentation[13,14]. Another family of PRRs that has frequently been exploited as an endocytic receptor to facilitate antigen cross-presentation are the C-type Lectin Receptors (CLRs). This family of PRRs recognizes carbohydrate patterns, and are an essential determinant in discerning host from foreign antigens. An often studied receptor is DC-SIGN (CD209), a CLR present on DCs that internalizes carbohydrate modified antigens for cross-presentation to T cells. DC-SIGN recognizes mannose and Lewis-type carbohydrate moieties on a wide variety of pathogens and is often targeted to activate specific signaling and tailor the immune response[15]. DC-SIGN can also act as a scavenger receptor that can induce receptor-mediated endocytosis. Due to its tetramic structure, a multivalent presentation of its ligand enhances the avidity for DC-SIGN. Thus, while the affinity for a single monomannoside ligand is low, targeting mannosylated constructs can be markedly increased by the multivalent presentation of the monosaccharides on a polyvalent core or carrier platform such as dendrimers, liposomes, or nanoparticles[16–18]. Vaccination with mannosylated antigens in mice has demonstrated improved cytotoxic lymphocyte responses, stronger Th1 and Th2 responses and increased antibody responses[19]. Addition of an adjuvant can further boost the generated immune response of mannosylated conjugates. For example, the conjugation of multivalent mannosides and TLR7 adjuvants to an antigen via a self-immolative linker resulted in a more robust and higher-quality humoral and cellular immune response in mice[20].

In earlier work, we have also demonstrated the significance of antigen mannosylation[21]. We systematically increased the number of well-defined mono-, di-, and tri-mannosides on a peptide backbone to evaluate the effect of multivalent presentation of DC-SIGN ligands on the peptide antigens. We could also extend the conjugates with a secondary adjuvant. Using this strategy, we generated precisely defined trifunctional conjugates (CLR-antigen-TLR), which effectively targeted DC-SIGN[21]. This approach however, required the conjugation of *O*-mannosides via a Cu(I) catalyzed azide-alkyne cycloaddition (CuAAC), which involved an additional purification step and limits the number of available orthogonal handles that can be incorporated into the conjugates. Furthermore, *O*-mannosides may be enzymatically cleaved rendering them less suitable for DC-SIGN targeting[16,22,23]. Therefore, we here report the design and synthesis of a *C*-mannose functionalized lysine building block (**1**, Scheme 1). This *C*-mannoside lacks the exo-cyclic anomeric oxygen to render the glycosidic linkage

resistant to the acidic conditions necessary for standard automated solid phase peptide synthesis (SPPS). Besides, the *C*-glycoside is resistant to enzymatic hydrolysis. By attachment to an Fmoc-protected amino acid building block, the mannoside can be incorporated *via* 'inline' synthetic methodology, obviating post-synthesis conjugation steps and preventing the use of an azide-alkyne click reaction. The *C*-mannoside building block has been used to generate peptide-antigen conjugates, carrying one or six mannosides, in addition to a synthetic TLR7 ligand. The generated constructs have been evaluated, in a side by side comparison to the corresponding *O*-mannoside clusters, for binding affinity, uptake and antigen presentation capacity, revealing that *C*-mannosides can effectively be used to replace their more labile *O*-counterparts in covalent antigen conjugates.

RESULTS AND DISCUSSION

Synthesis of the *C*-mannoside lysine building block

The synthesis of the key SPPS-ready mannosylated Fmoc amino acid is achieved in 11 steps and is shown in Scheme 1. The crucial step in the synthesis of **1** is the introduction of the α-*C*-glycosidic bond. Based on previously reported work by Girard *et al*.[24], the anomeric allyl was introduced *via* a Hosomi-Sakurai reaction using allyltrimethylsilane (allyl-TMS). The synthesis starts from methyl 2,3,4,6-tetra-*O*-benzyl-α-D-mannopyranoside **3**, obtained by benzylation of methyl α-D-mannopyranoside **2**[1]. The allyl group was introduced by treatment of the methyl mannoside with allyltrimethyl silane and trimethylsilyl triflate in acetonitrile to provide *C*-mannoside **4**. This reaction proceeded with high stereoselectivity and was complete within an hour when assisted by ultrasound irradiation[25]. Selective removal of the benzyl ethers in the presence of the allyl functionality was initially effected using either BCl_3 or a Birch reduction in liquid ammonia[26]. However, both reactions proved difficult to scale up and we therefore switched to the use of a single electron reduction using lithium naphthalenide in THF. This reaction could be run on 80 mmol scale, to provide the desired tetra-ol, which was acetylated to ease purification, delivering **5** in 54% yield. After the installation of four PMB ethers, the anomeric allyl appendage was elongated through a cross-metathesis with methyl acrylate to afford α,β-unsaturated ester **7**. The reduction of the double bond in this product with $RuCl_3$ in the presence of $NaBH_4$ and MeOH[27] was followed by saponification of the resulting ester **8** to obtain carboxylic acid **9**. Fully protected *C*-mannosyl lysine **12** was obtained by coupling of carboxylic acid **9** with the methyl ester of N_α-Fmoc protected lysine **11**, using HCTU as condensation agent. Selective hydrolysis of the ester in the presence of the Fmoc group was achieved with LiOOH[28,29], which is more nucleophilic but less basic than LiOH[30], resulting in the isolation of key building block **1** in 79% yield. Altogether, SPPS-compatible *C*-mannosyl **1** was synthesized in 20% yield over 11 steps.

[1] The use of per-acetylated mannosyl donors has previously shown to lead to anomeric mixtures, indicating that neighboring group participation falls short to effect stereoselective *C*-glycosylation reactions[21-25].

Scheme 1 Synthesis of *C*-mannoside lysine 1

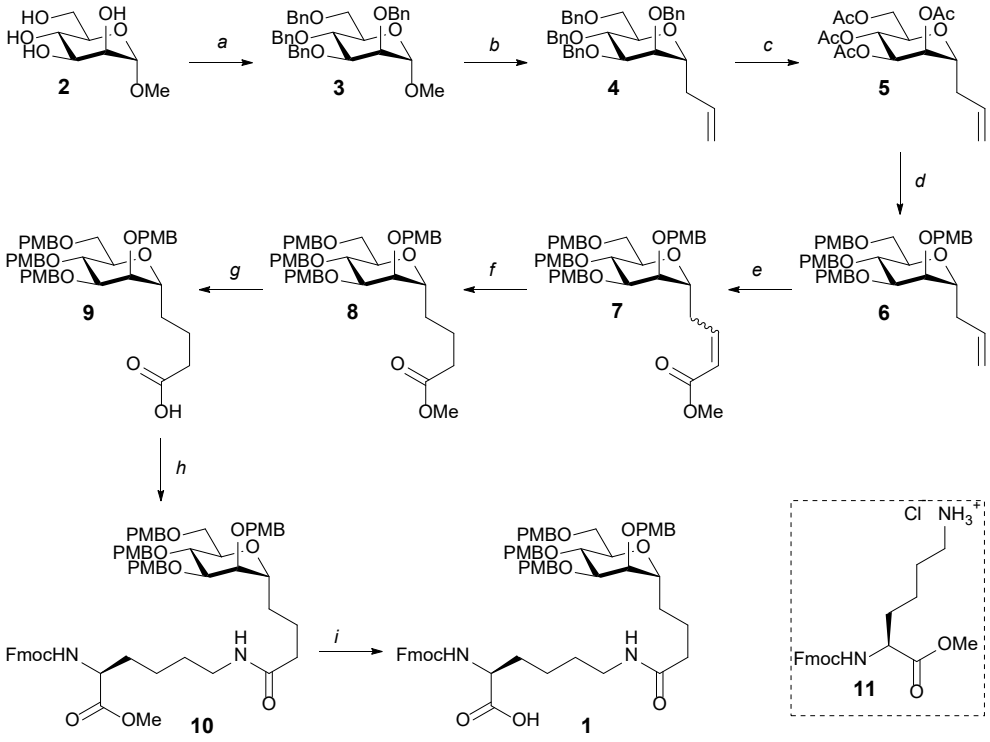

Reagents and conditions: a) NaH, BnBr, TBAI, DMF, 78%; *b)* allylTMS, TMSOTf, ACN, 73%; *c)* either *i.* BCl_3, DCM; *ii.* Ac_2O, pyridine 95% or *i.* Li, naphthalene, THF, -20°C; *ii.* Ac_2O, pyridine, 54%; *d) i.* NaOMe, MeOH; *ii.* NaH, PMBCl, TBAI, DMF, 69%; *e)* methyl acrylate, Grubbs 2nd gen. catalyst, DCM, 73%; *f)* $RuCl_3$, $NaBH_4$, DCE/MeOH, 93%; *g)* KOH, THF/H_2O, qnt.; *h)* **11**, HCTU, DIPEA, DMF, 99% ; *i)* LiOH, H_2O_2, THF/H_2O/*t*-BuOH, 79%.

Synthesis of the mannoside clusters

Our previous work has described the synthesis of the *O*-mannoside clusters[21], and resulted in monovalent- (**24**), bivalent- (**25**), trivalent- (**26**), and hexavalent (**27**) O-mannoside clusters. Biotinylation of these compounds resulted in biotinylated O-mannoside clusters **28**, **29**, **30**, and **31** respectively (Figure 1A). To enable the direct comparison to these clusters, we here generated clusters containing 1, 2, 3 or 6 copies of the *C*-mannosyl through an SPPS approach (Scheme 2). Using Tentagel® S RAM amide resin, Fmoc-Lys(Boc)-OH and Fmoc-Gly-OH were introduced successively, followed by elongation with *C*-mannosyl **1** using a standard Fmoc protocol and HCTU as the condensation agent. Building block **1** was introduced manually, using only a small excess of the amino acid and prolonged coupling times (2 eq, overnight) to prevent the use of a large excess of **1**. After completion of the sequence, the N-termini were capped with acetyl groups resulting in immobilized peptides **12-15**. Subjecting resins **12-15** to a cleavage cocktail of TFA/TIS/H_2O (190/5/5, v/v/v) successfully removed the Boc and PMB ethers and the peptide clusters were isolated after RP-HPLC purification to obtain monovalent- (**16**), bivalent- (**17**), trivalent- (**18**) and hexavalent- (**19**) clusters in 7%, 14%, 6%, and 2% yield respectively (Scheme 2, R = R_1). Further functionalization via the introduction of a biotin handle was achieved by reacting the primary amine of the C-terminal lysine with a biotin-N-

hydroxysuccinimide (NHS) ester. This resulted in biotinylated mannoside clusters **20-23** (Scheme 2, R = R_2).

Scheme 2 Synthesis of *C*-mannoside clusters

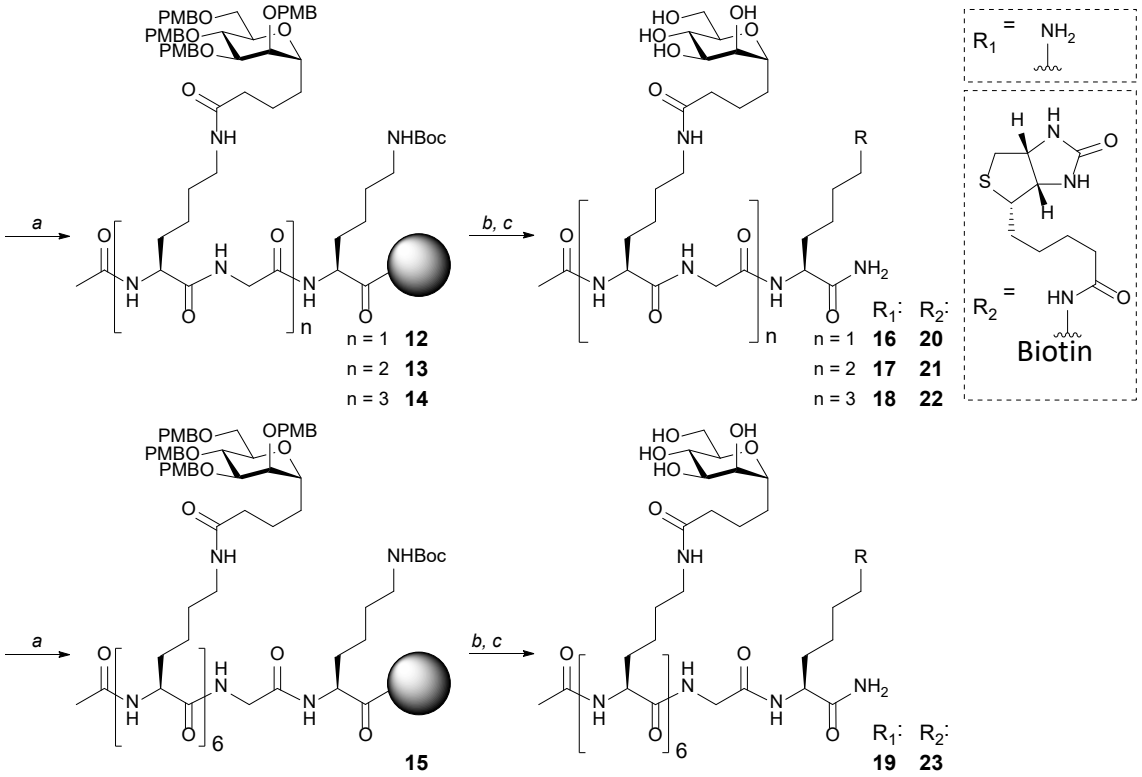

Reagents and conditions: a) Fmoc-SPPS (**1**, HCTU, DIPEA, DMF); *b)* TFA, TIS, H_2O, (octanethiol, phenol): (**16:** 7.0%; **17:** 14%; **18:** 6.0%; **19:** 2.1%); *c)* BiotinOSu, DIPEA, DMSO: (**20:** 94%; **21:** 72%; **22:** 99%; **23:** 80%).

Binding of the *C*-mannoside clusters to moDCs

With the biotinylated constructs in hand, the effect of the *O* to *CH_2* modification was evaluated by studying the binding, internalization and endosomal routing upon DC-SIGN engagement, of the *C*-mannoside clusters and their *O*-mannoside equivalents **28-31** (Figure 1A, 1B)[21]. The binding of the clusters to cellular membrane DC-SIGN was evaluated using DC-SIGN expressing monocyte-derived DCs (moDCs)(Figure 1C, also see Supporting Information, Figure SI.1A). The assay was performed at a temperature of 4°C to prevent the internalization of DC-SIGN from the cell membrane surface. The cells were incubated with the biotinylated clusters for 30 minutes, after which unbound clusters were washed away. Treatment of the cells with fluorophore-labeled streptavidin allowed quantification of binding by flow cytometry. An increase in binding of bivalent *C*-mannoside **21**, trivalent *O*-mannoside **30** and *C*-mannoside **22**, hexavalent *O*-mannoside **31** and *C*-mannoside **23** was seen when compared to the unstimulated control. Compared to a mannosylated polyacrylamide control, all compounds showed better binding, with the exception of mono-*O*-mannoside **28**. A clear valency-dependent increase in binding was seen within each of the *O*- and *C*-mannoside sets. These results are in line with our previous study, in which we compared the monomannoside clusters to clusters built up from more

complex di- and tri-mannosides[21]. For all clusters higher valency led to higher binding affininty. Binding of the hexavalent monomannoside cluster was comparable to the binding of the higher valent di- and trimannosides. Blocking of the DC-SIGN receptor effectively diminished the binding, although low residual binding with a similar valency-dependent increase remained (see SI, Figure SI.1B). The residual binding suggests cluster recognition of other mannose-binding receptors on DCs, such as mannose receptor[31].

We next selected the mono- and hexavalent *O*- and *C*-mannoside clusters to assess their internalization. The assessment of cluster internalization was executed at 4°C, similar to the binding assay. To this end, the cells were incubated for 60 minutes to saturate the immobilized DC-SIGN receptors at the cell surface, followed by the removal of unbound clusters. Re-suspension of the samples in warm (37°C) medium initiated internalization. At the indicated time points, samples were taken and immediately put on ice. The signal loss of the membrane was measured through flow cytometry upon treatment with a fluorophore-conjugated streptavidin. To exclude cluster-DC-SIGN dissociation, we additionally gently fixed the cells with 1% paraformaldehyde for permanent immobilization of DC-SIGN at the membrane. No dissociation of the mannosylated clusters from DC-SIGN on fixed cells was measured (see SI, Figure SI.1C), indicating that the ligands are internalized upon DC-SIGN binding. Internalization (>50%) of the hexavalent cluster **23** was seen after 5 minutes (Figure 1D). The complementary *O*-mannoside cluster (**31**) accomplished the same level of internalization after 15 minutes. Uptake of the monovalent clusters occurred at a slower rate, requiring 30 minutes for internalization of approximately 50% of both the *O*- and *C*-mannose clusters (**28**, **20**). The relative internalization efficiency seems to mirror the binding profiles seen in Figure 1C.

Mono- and hexavalent cluster trafficking to the endosomes was further studied using pHrodo® Red. This dye acts as a pH-sensitive sensor, as the fluorescence is considerably increased in acidic environments, while it is quenched in the neutral extracellular environment. Prior to moDC stimulation, the biotinylated mannoside clusters were treated with the avidin-conjugated fluorophore (2:1). The pre-complexed clusters were subsequently added to the moDCs at 37°C, continued by sample collection at each time point. The cells were washed, gently fixed, and fluorescence was subsequently measured by flow cytometry. After 30 minutes, a 2-fold increase was visible in the fluorescence of the hexavalent *O*- and *C*-mannoside clusters (Figure 1E). On the other hand, the fluorescence of both monovalent clusters (**28** and **20**) was increased 2.5-folds at 30 minutes, suggesting higher endosomal ligand concentrations. Although the *C*-mannosides resembled the *O*-mannoside clusters, the deviation between mono- and hexavalent presentation is surprising. In the previous binding and internalization assays, the hexavalent clusters **31** and **23** were superior to monovalent mannoside presentation. The increased MFI of the monovalent over the hexavalent clusters at 30 minutes could indicate faster endo-lysosomal trafficking of the smaller clusters, as the emitted fluorescence by the dye is higher with lower pH[32,33]. Moreover, the mannosylated clusters were pre-complexed with the pHrodo dye into a larger particle, possibly contributing to the altered endocytosis[34]. Altogether these results indicate that the *C*-mannoside clusters **20** and **23** were able to convincingly resemble the DC-SIGN binding[16] and internalization profiles of the *O*-mannoside equivalents, encouraging the implementation of *C*-mannosylated antigen conjugates.

Figure 1 Binding of the *C*-mannoside clusters to DC-SIGN

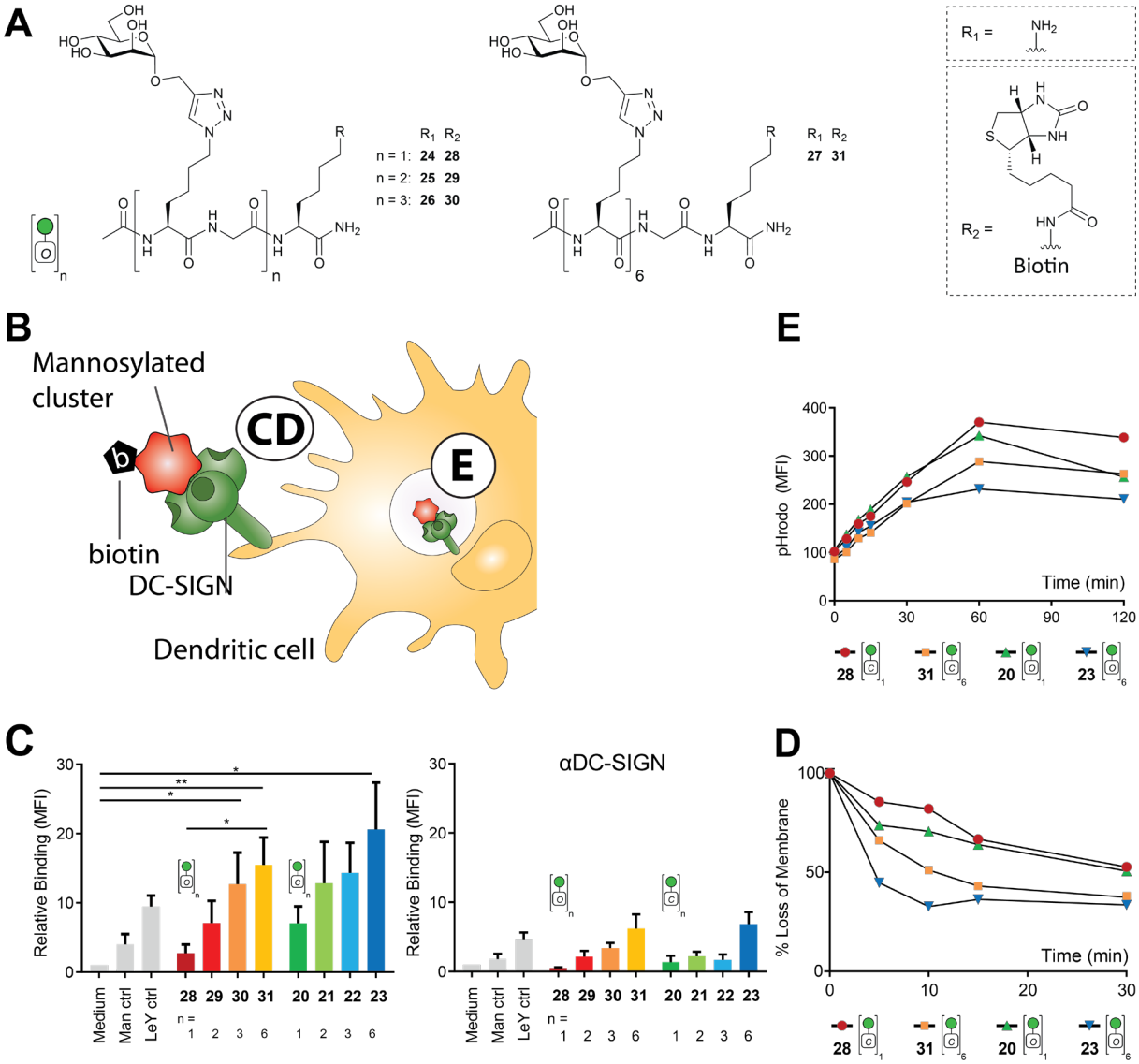

(A) Structure of the mono-, di-, tri-, or hexavalent *O*-mannoside clusters, with and without biotin. (B) Schematic representation of the binding, internalization, and endosomal routing assays. (C) Binding of the biotinylated clusters to moDC DC-SIGN as measured by flow cytometry (left panel, eight donors), and to moDC with blocked DC-SIGN (right panel). Polyacrylamide decorated with monomannosides or Le^Y antigens were used as positive control. Paired Student's t-test error: *, $p < 0.05$; **, $p < 0.001$. (D) DC-SIGN-mediated internalization of the clusters was measured by flow cytometry. One donor is depicted as a representative of four individuals. (E) The routing of the clusters to the endosomes/lysosomes as measured by flow cytometry and normalized to a negative control. One donor is depicted as representative of three individuals.

Synthesis of mannosylated gp100 conjugates

Melanoma derived from transformed pigment-carrying melanocytes is a highly lethal cancer, and this malignancy is considered one of the most immunogenic cancer types[35]. We therefore selected the

melanoma-associated antigen gp100 as our vaccine target, and we introduced C-terminal mannoside clusters and a secondary TLR ligand to generate self-adjuvating peptide antigen vaccine conjugates[36]. Endosomal TLR7 was selected as PRR-target because we reasoned that the use of a cell surface PRR targeting PAMP would lead to competition for binding with DC-SIGN on the outside of the DC surface membrane. Furthermore, DC-SIGN-mediated endocytosis should deliver the conjugates to the endosomes, where it will encounter the TLR7 receptor. The target gp100 peptide antigen combines the $CD4^+$ T cell binding epitope $gp100_{280\text{-}288}$ and $CD8^+$ T cell binding epitope $gp100_{44\text{-}59}$. Multiple conjugates were synthesized bearing the TLR7 agonist either on the N- or C- terminus and carrying either one or six mannosides, to study the effect of these modifications on antigen presentation.

The SPPS of the conjugates started with the introduction of a monomethoxytrityl (Mmt) functionalized Fmoc-Lys-OH on Tentagel® S RAM amide resin (Scheme 3). Both termini of the antigen sequence were extended with four naturally occurring amino acids to act as spacers between the antigens, the mannoside cluster, and the TLR7 ligand. The Cys_{60} in the N-terminal spacer was replaced with an isosteric α-amino-butyric acid analog to prevent potential oxidation and peptide dimerization[37], a modification we previously demonstrated not to affect antigen biology[21]. The sequences were elongated at the *N*-terminus with either one or six copies of the *C*-mannosyl **1**, resulting in immobilized peptides **33** and **34** (Scheme 3). Next, **33** and **34** were further extended at their *N*-termini with the TLR7 ligand 2-butoxy-8-oxo-adenine, using the previously described Boc protected building block **32**[38], to give immobilized conjugates **35** and **36**. Alternatively, the *N*-termini were acetylated, after which the *C*-termini were further functionalized by selective removal of the *C*-terminal lysine Mmt-group, followed by the introduction of the TLR7 ligand to provide **37** and **38**[39]. It was observed that a cocktail of TFA (1%) in DCM, led to partial removal of the PMB groups leading to the undesired esterification of some of the carbohydrate alcohols with the TLR7 ligand. Therefore, milder conditions were explored for the removal of the *C*-terminal Mmt-group. Eventually, the use of acetic acid in a mixture of trifluoroethanol (TFE) and DCM (1/2/7, v/v/v), a cocktail first described to selectively cleave the Mmt over methyltrityl and trityl-groups selectively[40], was found to be effective for the selective unmasking of the MMT in the resin-bound protected conjugates. Using these conditions, the immobilized N-terminal elongated conjugates **37** and **38** were successfully generated.

Initial attempts to deprotect and release the peptides from the resin with a cleavage cocktail of TFA/TIS/H_2O (190/5/5, v/v/v) resulted in complex crude mixtures. Analysis of the mixtures indicated that the poor quality of the crude material was due to side reactions of the cleavage and deprotection step and not due to incomplete couplings. Reactive cationic species are liberated during the acidic removal of the PMB ethers, which can react with functional groups in the unprotected peptide[41]. Howard *et al.*[42] effectively scavenged PMB-cations using phenol as an electron-rich aromatic additive, and when this additive was applied here, the quality of the crude mixture indeed improved. Further optimization of the cleavage conditions was achieved by increasing the concentration of the scavengers (up to 10% of the total volume) and increasing the volume of cleavage medium (effectively diluting the concentration of reactive cationic species and reactive functional groups). Using this optimized cleavage protocol all four peptides were successfully deprotected and released form the resin. After RP-HPLC purification, the monovalent *C*-mannose conjugate **39** was obtained in 2.6% yield after 36 couplings steps and the hexavalent *C*-mannose conjugate **40** in 1.3% yield over 41 couplings. The conjugates **41** and **42** were isolated in 2.1% (after 36 steps) and 0.6% (after 41 couplings), respectively (Scheme 3). Unlike the *O*-mannoside conjugates, we previously generated, these constructs did not require additional conjugation and purification steps.

To compare the activity of the *C- vs.* the *O*-mannoside conjugates, *O*-mannoside clusters **24** and **27** were functionalized with an alkyne handle (yielding **43** and **44**) and conjugated through a CuAAC ligation to the TLR7L- gpl00 peptide **45** to obtain analogs **46** and **47**.

Scheme 3 Synthesis of C- and O- mannoside – gp100 – TLR7 agonist conjugates

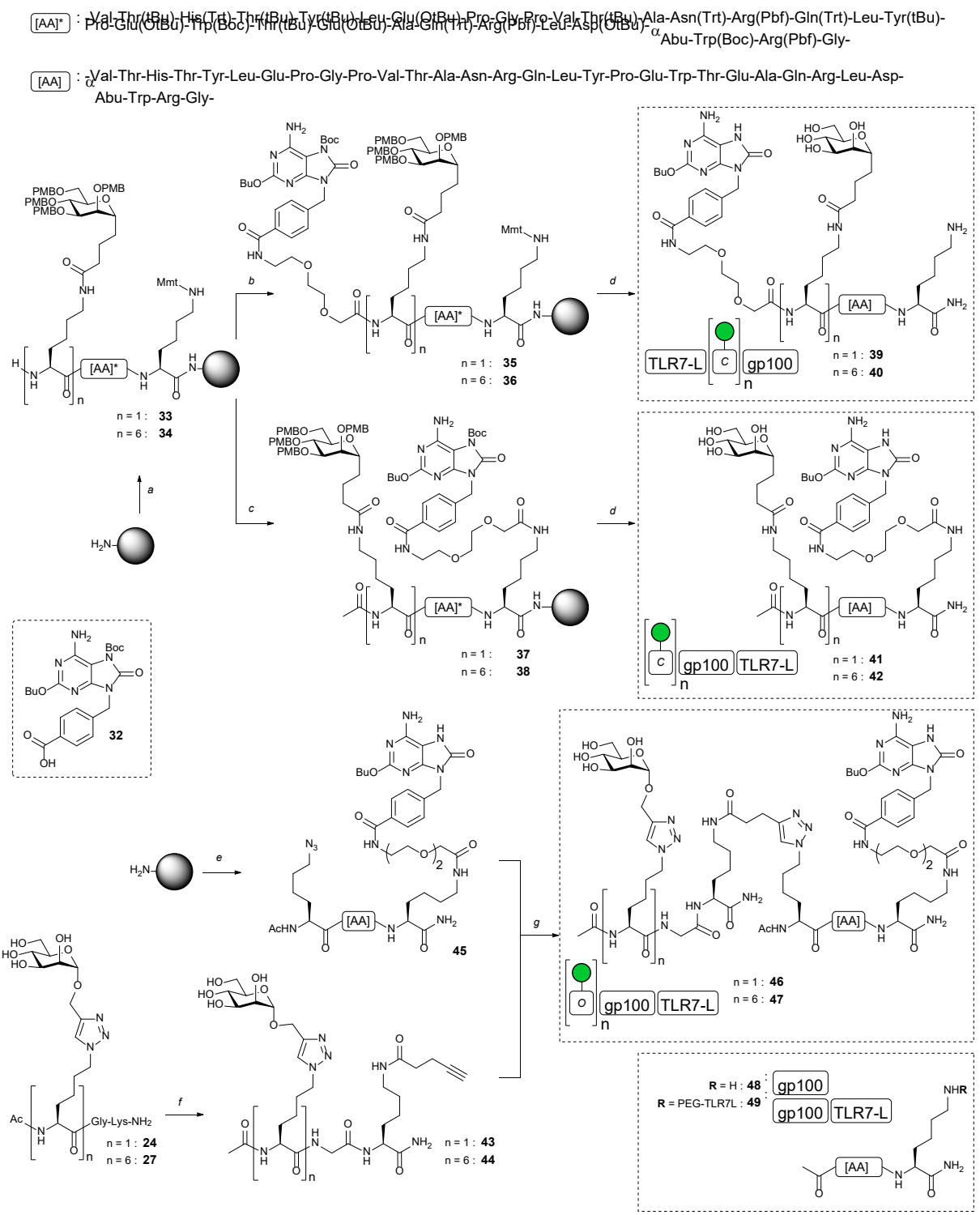

Reagents and conditions: a) Fmoc-SPPS (**1**, HCTU, DIPEA, DMF); *b)* Fmoc-SPPS (Fmoc-AEEA-OH or **32**, HCTU, DIPEA, DMF); *c) i.* Ac_2O, DIPEA, DMF; *ii.* AcOH, TFE, DCM; *iii.* Fmoc-SPPS (Fmoc-AEEA-OH or **32**, HCTU, DIPEA,

DMF); *d)* TFA, TIS, H_2O, octanethiol, phenol: (**39:** 2.60% over 36 couplings; **40:** 1.30 % over 41 couplings); **41:** 2.10% over 36 couplings); **42:** 0.60% over 41 couplings; *e)* Fmoc-SPPS see reference[21]; *f)* Pent-4-ynoic acid succinimidyl ester, DIPEA, DMSO: (**43**: 62%; **44**: 66%); *g)* CuI, THPTA, DIPEA, H_2O, DMSO: (**46**: 34%; **47**: 29%).

Mannosylated gp100 conjugate efficacy as vaccination strategy

We analyzed the influence of the *C*-mannosylated antigens on dendritic cell maturation, cytokine secretion, and antigen presentation to $CD4^+$ and $CD8^+$ T lymphocyte in relation to their *O*-mannosylated peptide counterpart (Figure 2A). Furthermore, the effect of C- versus N- terminal ligation of the TLR7 ligand was assessed.

Dendritic cell maturation is considered an essential requirement for proper T lymphocyte activation and polarization. As a measure of DC maturation, we quantified expression of the co-stimulatory molecules CD86 (Figure 2B) and CD83 (see SI, Figure SI.1D) using the six variants of the trivalent conjugates. The non-glycosylated gp100 **48** and the bivalent gp100-TLR7L conjugate **49** were included as controls. After overnight stimulation with the conjugates, we found that all conjugates induced expression of CD86 and CD83. The *C*-mannoside conjugates did not hamper the DC maturation processes and effectively elevated expression levels to the same extent as the *O*-mannosylated conjugates. The position to which the TLR7 agonist was attached does not seem to affect the maturation of the DCs in this assay.

During maturation, DCs produce and secrete a tailored cytokine cocktail for subsequent T lymphocyte skewing. The secreted cytokine profile depends on the triggered TLR, the signaling pathway of which can be modified by DC-SIGN or other CLR engagement[43]. To assess DC activation, we quantified four key cytokines using a sandwich ELISA. IL-6 and IL-12 are primarily characterized as pro-inflammatory cytokines, with functions aiding DC maturation and Th1 stimulation, respectively. Tumor necrosis factor (TNF)-α is required for DC activation and proliferation, and reduces IL-10 mediated inhibition during DC development[44]. IL-10 is a cytokine that interferes with DC maturation and inhibits the production of IL-12, and as such has been implied to play a role in skewing of naïve T lymphocytes to Treg differentiation[45]. Low levels of autocrine IL-10 prevent spontaneous maturation of DCs[46]. Figure 2C shows that the stand-alone peptide (**48**) and gp100-TLR7L (**49**) minimally induced the production of IL-6, while both the monovalent and hexavalent *O*-mannoside trifunctional conjugates **46** and **47** increased the secretion of this pro-inflammatory cytokine. The monovalent and hexavalent *C*-mannoside conjugates **41** and **42** increased the IL-6 levels to a similar extent as their *O*-mannoside counterparts. However, when moDCs were stimulated with conjugates **39** and **40**, having both the *C*-mannosides and the TLR7L attached to the *N*-terminus of the peptide sequence, cytokine production was abrogated. A similar pattern observed for the IL-12 production profile: the *O*- and *C*-mannose conjugates having the TLR7 ligand at the C-terminus of the conjugate were most active in stimulating the production of this cytokine, while the gp100 peptide and gp100 peptide-TLR7L conjugate were less active. The conjugates **39** and **40** induced low levels of the IL-12 cytokine. TNF-α expression levels were minimally affected upon stimulation of the DCs with the various conjugates. Also here, the conjugates carrying the TLR7 ligand and the mannosides at the same side of the peptide antigen showed least activation. Finally, a low level of the anti-inflammatory IL-10 was detected in the ELISA with the non-stimulated DCs, as well as for those treated with peptide **49**. Figure 2C shows that while LPS effectively

triggers the production of IL-10, the mannosylated conjugates do not induce the production of this cytokine. Overall the cytokine production profiles of the *O*- and *C*-mannose conjugates appear to be very similar for both the monovalent and hexavalent clusters. In addition, these experiments revealed that the arrangement of the CLR and TLR ligands within the trifunctional conjugates has a great influence on the activity of the conjugates. Possibly, the processing of these conjugates is different from the conjugates bearing the CLR and TLR ligand on either side of the conjugate, due to differential cleavage of the conjugates by proteases.

Finally, we studied the antigen presentation capacity of the DCs upon stimulation with all the trifunctional conjugate variations. During DC maturation, the intrinsic focus of these cells shifts from antigen endocytosis to antigen processing, major histocompatibility complex (MHC) molecule loading, and presentation of the antigens for initiation of the T cell response. Upon recognition of the cross-presented antigen in MHC-I, cytotoxic $CD8^+$ T cells induce programmed cell death of targeted cells. On the other hand, $CD4^+$ T lymphocytes induce and support a cellular and humoral response upon antigen-MHC-II binding. As both T-cell responses are needed for a robust immune response, we studied the antigen (gp100) presenting capacity of the DCs to both $CD8^+$ and $CD4^+$ T cells after stimulation with the trifunctional conjugates[47]. To this end, DCs were stimulated for 30 minutes with the conjugates, before washing and co-culturing with the $CD8^+$ HLA-A2.1 or $CD4^+$ HLA-DR4.1 restricted T cell clone for 24 hours. Activation of T cells was measured by quantification of the IFNγ cytokine produced. As shown in Figure 2D, the conjugates carrying a TLR7 ligand are more active than the stand-alone peptide, except for conjugate **40**. The introduction of a CLR ligand also increases the antigen-presenting activity of the conjugates, although the hexavalent *C*-mannoside conjugate appears to hamper antigen presentation with respect to the monovalent conjugate partially. The presence of the TLR7 ligand and the hexavalent mannoside cluster on the same side of the conjugate blocks $CD8^+$ antigen presentation, likely as the result of sub-optimal processing. In our previous study, in which we have investigated gp100-conjugates bearing hexavalent clusters comprising di- and trimannosides we found that the α1,2-dimannoside cluster gp100 conjugates, although being the best DC-SIGN binders, showed less antigen presentation than a gp100-TLR7 conjugate lacking the carbohydrate cluster. Clusters composed of α1,3- and α1,6-linked dimannosides or α1,3-α1,6-linked trimannosides showed slightly enhanced antigen presentation. Taken together, these results show that optimal antigen presentation requires not only DC-SIGN binding but also adequate processing of the incorporated antigens. These results were substantiated by the $CD4^+$ T cell activation assay, as similar gp100 antigen presentation effects were seen (Figure 2E).Monovalent *O*- and *C*-mannosyl conjugates **46** and **41** improved antigen presentation to $CD4^+$ T cells most, and attachment of the TLR7 ligand to the same side as the CLR ligand again nullified activity of the conjugates. Overall, also in these assays, the *O*- and *C*-mannosides perform similarly. The combined results from the assays in Figure 2 show that the most attractive vaccine conjugates require the antigenic peptide to be placed between an *N*-terminal CLR ligand and a C-terminal TLR-ligand for antigen presentation and secretion cell activation.

Figure 2 targeting efficacy of the mannoside-peptide conjugates

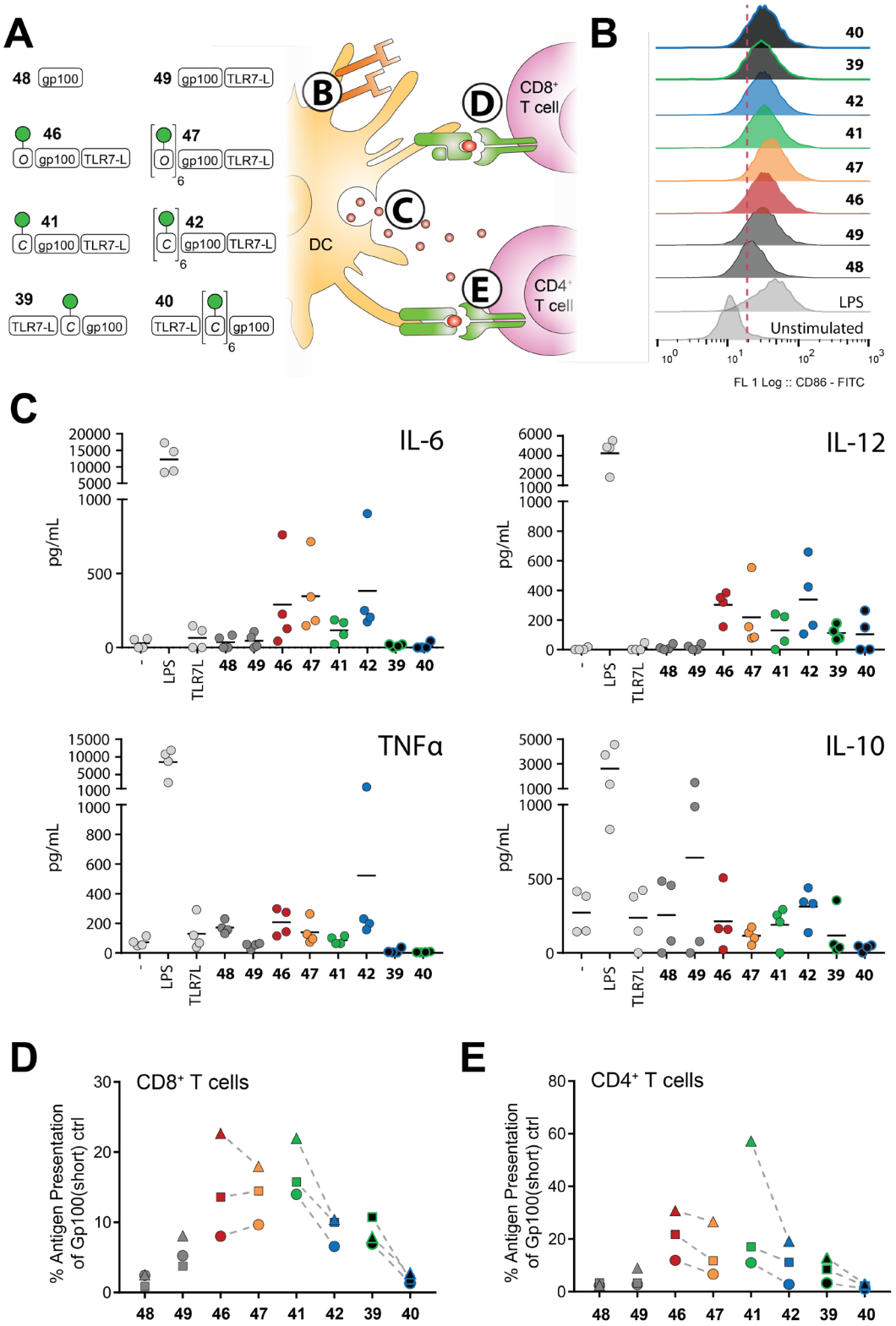

(A) Schematic representation of the compounds and overview of the moDC maturation, cytokine secretion, CD4⁺ and CD8⁺ T lymphocyte antigen presentation. (B) Expression of co-stimulatory marker CD86 as measured by flow cytometry. One out of four donors is depicted. LPS and **49** were included as positive controls, as well as **48** as a negative control. (C) IL-6, IL-10, IL-12p70, and TNFα secretion of four donors was measured using ELISA upon overnight stimulation with *O*- or *C*-mannoside conjugates. (D) Antigen presentation capacity of moDCs to CD8⁺ T lymphocytes was quantified by the IFNγ production of activated T cells. The dashed lines represent the directionality between the donors when

comparing mono and hexavalent mannosides analogs. (E) Antigen presentation capacity of moDCs to $CD4^+$ T lymphocytes was quantified by the IFNγ production of activated T cells.

CONCLUSION

In conclusion, we have developed a *C*-mannosyl lysine that can be effectively used in solid-phase peptide synthesis (SPPS) campaigns. The stability of the *C*-glycosidic linkage renders the mannoside stable to both acidic reaction conditions employed during SPPS and enzymatic degradation. The protecting groups on the building block were designed to be compatible with standard SPPS protocols to allow the straightforward 'in-line' incorporation of the mannosylated residues in oligopeptides. This allows for the generation of mannosylated conjugates without the necessity of a post-assembly conjugation step requiring orthogonal click strategies. Not only does this streamline the synthesis of these conjugates, it also ensures that bio-orthogonal handles, such as azides and alkynes, can be incorporated into these multifunctional antigen-conjugates to allow these for the incorporation of additional functionalities, such as other immune stimulating agents or fluorophores. We have applied the mannosylated lysine in the assembly of a set of synthetic long peptide antigens to equip these with either one or six mannosides to target the antigens to mannose-binding C-type lectins on professional antigen-presenting cells to improve the antigenicity of the peptides. The conjugates were further armed with a synthetic TLR7 ligand to further boost the response against the antigens. In comparing the *C- vs.* the *O*-mannosylated conjugates for DC-SIGN mediated uptake, DC-maturation, and stimulation as well as $CD4^+$ and $CD8^+$ antigen presentation, the stabilized mannosides performed virtually identical to their natural analogs. The conjugates bearing the mannosides and a TLR7 ligand were shown to bind DC-SIGN and activate DCs, as indicated by pro-inflammatory cytokine release, upregulation of cell surface maturation markers and increased antigen presentation to both $CD4^+$ and $CD8^+$ lymphocytes. Notably, the relative position of the CLR and TLR ligands in the peptide antigen conjugates played an important role in shaping the activity of the conjugates. The conjugates bearing the mannose cluster and the TLR7 ligand on the same side of the conjugates proved to be poor immune-stimulating agents, incapable of elucidating an effective pro-inflammatory response and showing poor antigen presentation. These differences are likely due to differences in the processing of the conjugates. As DC vaccination therapies hold great promise as an immunotherapeutic approach to fight cancer, the development of more effective, tailor-made cancer vaccine conjugates, of which the action is well understood and can be controlled, is of great importance. The conjugates described here can be further equipped with biorthogonal visualization handles to allow tracking of the conjugates during uptake and processing. Because the *C*-mannosyl lysine building block can be incorporated in an 'in-line' manner and does not rely on a post-assembly conjugation step, often used biorthogonal coupling partners, such as azides and alkynes, remain at one's disposal for inclusion in the conjugates.

METHODS

Synthesis

The synthesis of C-mannosyl **1** and all clusters and conjugates is described in the Supporting Information.

Cell isolation and culture

Buffy coats of healthy donors were obtained from Sanquin Amsterdam (reference: S03.0023-XT). Monocytes were isolated using a Ficoll (STEMCELL Technologies) and sequential Percoll (Sigma) gradient centrifugation. The monocytes were differentiated to monocyte-derived dendritic cells (moDCs) in RPMI 1640 (Invitrogen), supplemented with 10% FCS (Biowittaker), 1.000 U/mL penicillin (Lonza), 1 U/mL streptomycin (Lonza), 262.5 U/mL IL-4 (Biosource), and 112.5 U/mL GM-CSF (Biosource), for five days. Flow cytometric monitoring of DC-SIGN (AZN-D1-Alexa488, in house[48]), CD83 and CD86 (both PE-conjugated, Becton Dickinson) expression was conducted for every donor.

Binding of the mannose clusters to moDCs

Day 5 moDCs (approximately 10^5 per condition) were washed and resuspended in ice-cold RPMI medium (Invitrogen). The entire experiment was conducted at 4°C with pre-cooled reagents. DC-SIGN and mannose receptor were blocked with 20 µg/mL AZN-D1 (in house[48]) or purified mouse anti-human CD206 antibody (Clone 19.2, BD Bioscience) respectively for 45 minutes. The biotinylated mannoside clusters (10 µM) or Lewis^Y-conjugated polyacrylamide (1 µg/mL) as positive control was allowed to bind for 30 minutes. The moDCs were washed with PBS and stained with an Alexa647-labelled streptavidin (Invitrogen™) in PBS supplemented with 0.5% BSA and 0.02% NaN_3 (PBA) for 30 minutes. The moDCs were subsequently washed and fixed in PBS with 0.5% PFA, before the fluorescence was measured by flow cytometry (CyAn™ ADP with Summit™ Software), and analyzed using FlowJo v10.

Internalization of the mannoside clusters

Day 5 moDCs (approximately 10^5 per condition) were washed and resuspended in ice-cold HBSS medium (Thermo Fischer). The biotinylated mannoside clusters (20 µM) were added in ice-cold medium to the moDCs for one hour, and washed away with ice-cold medium. Pre-warmed HBSS (37°C) was added to the cells and were incubated at 37°C in a shaking heating block (800 RPM). Samples of the cells were taken at the indicated time points (t = 0, 5, 10, 15, 30, 60 minutes), and immediately put on ice. The moDCs were washed with ice-cold PBS supplemented with 0.5% BSA and 0.02% NaN3 (PBA) and stained with Alexa647-labelled streptavidin (InvitrogenTM) for 30 minutes at 4°C. The fluorescence was measured by flow cytometry (CyAn™ ADP with Summit™ Software), and analyzed using FlowJo v10.

Endosomal routing of the mannoside clusters

Day 5 moDCs (approximately 10^5 per condition) were washed and resuspended in pre-warmed (37°C) HBSS medium (Thermo Fischer). The biotinylated mannoside clusters (20 µM) were complexed with pHrodo (2:1 ratio) for 15 minutes at RT. The pre-complexed pHrodo-labeled ligands were added to the cells and were incubated at 37°C in a shaking heating block (800 RPM). Samples of the cells were taken at the indicated time points (t = 0, 5, 10, 15, 30, 60, 120 minutes), and immediately put on ice. The moDCs were washed with ice-cold PBS supplemented with 0.5% BSA and 0.02% NaN3 (PBA). The fluorescence was measured by flow cytometry (BD LSRFortessa™ X-20 with FACSDiva Software), and analyzed using FlowJo v10.

moDC Cytokine secretion upon stimulation with the mannoside clusters

Day 5 moDCs (approximately $50 \cdot 10^5$ per condition) were stimulated for 24 hours with the trifunctional conjugates. Cytokines IL-6, IL-10, IL-12p40, and TNFα in the supernatant were measured by sandwich ELISA according to manufacturer's protocol (Biosource). The capture antibody was coated in NUNC MaxiSorp plates (Nunc, Roskilde, Denmark) overnight at 4°C in PBA-0.05% BSA. The plates were

blocked for 30 minutes at 37°C, using PBS supplemented with 1% BSA. Samples were added for 2 hours at RT to allow binding, subsequently washed, and cytokine levels were detected using a peroxidase-conjugated cytokine-specific detection antibody. After extensive washing, the binding was visualized with 3,3',5,5'-tetramethylbenzidine (Sigma Aldrich) and measured by spectrophotometry at 450 nm on the iMark™ Microplate Absorbance Reader (Bio-RAD).

$CD4^+$ and $CD8^+$ Antigen presentation

Day 5 moDCs of HLA-A2 and HLA-DR4 double positive donors (approximately $40{\cdot}10^3$ per condition) were incubated with the different trifunctional conjugates (20 μM) for 30 minutes at 37°C. A short gp100 peptide ($gp100_{280\text{-}288}$) and a long gp100 peptide ($gp100_{280\text{-}288,\ 40\text{-}59}$) were used as controls. The moDCs were washed and separated into two plates ($30{\cdot}10^3$ for $CD8^+$ and $10{\cdot}10^3$ for $CD4^+$ T lymphocyte co-culture). Either a $CD8^+$ HLA-A2.1 restricted T cell clone transduced with the TCR specific for the $gp100_{280–288}$ peptide[49] (approximately 10^5 cells per condition, E:T ratio 1:3) or a $CD4^+$ HLA-DR4.1 restricted T cell clone transduced with the TCR specific for the $gp100_{44\text{-}59}$ peptide (approximately 10^5 cells per condition, E:T ration 1:10) was added for overnight co-culture. The interferon γ cytokine secretion was measured by sandwich ELISA, according to the manufacturer's protocol (Biosource), and measured by spectrophotometric analysis at 450 nm on the iMark™ Microplate Absorbance Reader (Bio-RAD).

Statistics

Unless otherwise stated, data are presented as the mean ± SD of at least three independent experiments or healthy donors. Statistical analyses were performed in GraphPad Prism v7.04. Statistical significance was set at $P < 0.05$ and it was evaluated by the Mann–Whitney U test.

Supporting information

All other synthetic procedures, supporting figures, NMR spectra and HPLC spectra are depicted in the Supporting Information.

6 Author information

6.1 Corresponding Author

*E-mail: JCodee@chem.leidenuniv.nl

*E-mail: Y.vanKooyk@amsterdamumc.nl

6.2 ORCID

Tim Hogervorst: https://orcid.org/0000-0002-4686-6251
R.J. Eveline Li: https://orcid.org/0000-0002-1928-925X
Yvette van Kooyk: https://orcid.org/0000-0001-5997-3665
Jeroen Codée: http://orcid.org/0000-0003-3531-2138

6.3 Author Contributions

TH and RL equally contributed to the work and both wrote the manuscript. The compounds were synthesized by TH, assisted by LM, under the supervision of HO, DF, GM, and JC. NM aided in the

peptide synthesis and purification of certain constructs. RL executed the binding, internalization, endosomal tracking, maturation, and cytokine secretion experiments, and was assisted by SB in the antigen presentation assay, supervised by SV and YK.

Notes

All authors declare that the research was conducted in the absence of any commercial or financial relationships that could be construed as a potential conflict of interest.

Acknowledgements/Funding

This work was funded by the NWO gravitation program 2013 granted to the Institute for Chemical Immunology (ICI-024.002.009).

References

(1) Khair, D. O.; Bax, H. J.; Mele, S.; Crescioli, S.; Pellizzari, G.; Khiabany, A.; Nakamura, M.; Harris, R. J.; French, E.; Hoffmann, R. M.; Williams, I. P.; Cheung, A.; Thair, B.; Beales, C. T.; Touizer, E.; Signell, A. W.; Tasnova, N. L.; Spicer, J. F.; Josephs, D. H.; Geh, J. L.; MacKenzie Ross, A.; Healy, C.; Papa, S.; Lacy, K. E.; Karagiannis, S. N. Combining Immune Checkpoint Inhibitors: Established and Emerging Targets and Strategies to Improve Outcomes in Melanoma. *Front. Immunol.* **2019**, *10*, 453.

(2) Boyiadzis, M. M.; Dhodapkar, M. V.; Brentjens, R. J.; Kochenderfer, J. N.; Neelapu, S. S.; Maus, M. V.; Porter, D. L.; Maloney, D. G.; Grupp, S. A.; Mackall, C. L.; June, C. H.; Bishop, M. R. Chimeric Antigen Receptor (CAR) T Therapies for the Treatment of Hematologic Malignancies: Clinical Perspective and Significance. *J. Immunother. Cancer* **2018**, *6*, 137.

(3) Rohaan, M. W.; van den Berg, J. H.; Kvistborg, P.; Haanen, J. B. A. G. Adoptive Transfer of Tumor-Infiltrating Lymphocytes in Melanoma: A Viable Treatment Option. *J. Immunother. Cancer* **2018**, *6*, 102.

(4) Huber, A.; Dammeijer, F.; Aerts, J. G. J. V; Vroman, H. Current State of Dendritic Cell-Based Immunotherapy: Opportunities for in Vitro Antigen Loading of Different DC Subsets? *Front. Immunol.* **2018**, *9*, 2804.

(5) Schreibelt, G.; Bol, K. F.; Westdorp, H.; Wimmers, F.; Aarntzen, E. H. J. G.; Duiveman-de Boer, T.; van de Rakt, M. W. M. M.; Scharenborg, N. M.; de Boer, A. J.; Pots, J. M.; Olde Nordkamp, M. A. M.; van Oorschot, T. G. M.; Tel, J.; Winkels, G.; Petry, K.; Blokx, W. A. M.; van Rossum, M. M.; Welzen, M. E. B.; Mus, R. D. M.; Croockewit, S. A. J.; Koornstra, R. H. T.; Jacobs, J. F. M.; Kelderman, S.; Blank, C. U.; Gerritsen, W. R.; Punt, C. J. A.; Figdor, C. G.; de Vries, I. J. M. Effective Clinical Responses in Metastatic Melanoma Patients after Vaccination with Primary Myeloid Dendritic Cells. *Clin. Cancer Res.* **2016**, *22*, 2155–2166.

(6) Anguille, S.; Smits, E. L.; Lion, E.; van Tendeloo, V. F.; Berneman, Z. N. Clinical Use of Dendritic Cells for Cancer Therapy. *Lancet Oncol.* **2014**, *15*, e257–e267.

(7) Ho, N. I.; Huis in 't Veld, L. G. M.; Raaijmakers, T. K.; Adema, G. J. Adjuvants Enhancing Cross-Presentation by Dendritic Cells: The Key to More Effective Vaccines? *Front. Immunol.* **2018**, *9*, 2874.

(8) Blander, J. M.; Medzhitov, R. Toll-Dependent Selection of Microbial Antigens for Presentation by Dendritic Cells. *Nature* **2006**, *440*, 808–812.

(9) Cho, H. J.; Takabayashi, K.; Cheng, P.-M.; Nguyen, M.-D.; Corr, M.; Tuck, S.; Raz, E. Immunostimulatory DNA-Based Vaccines Induce Cytotoxic Lymphocyte Activity by a T-Helper Cell-Independent Mechanism. *Nat. Biotechnol.* **2000**, *18*, 509–514.

(10) Deres, K.; Schild, H.; Wiesmüller, K.-H.; Jung, G.; Rammensee, H.-G. In Vivo Priming of Virus-Specific Cytotoxic T Lymphocytes with Synthetic Lipopeptide Vaccine. *Nature* **1989**, *342*, 561–564.

(11) Fujita, Y.; Taguchi, H. Overview and Outlook of Toll-like Receptor Ligand–Antigen Conjugate Vaccines. *Ther. Deliv.* **2012**, *3*, 749–760.

(12) Willems, M. M. J. H. P.; Zom, G. G.; Khan, S.; Meeuwenoord, N.; Melief, C. J. M.; Stelt, M. van der; Overkleeft, H. S.; Codée, J. D. C.; Marel, G. A. van der; Ossendorp, F.; Filippov, D. V. N - Tetradecylcarbamyl Lipopeptides as Novel Agonists for Toll-like Receptor 2. *J. Med. Chem.* **2014**, *57*, 6873–6878.

(13) Ignacio, B. J.; Albin, T. J.; Esser-Kahn, A. P.; Verdoes, M. Toll-like Receptor Agonist Conjugation: A Chemical Perspective. *Bioconjug. Chem.* **2018**, *29*, 587–603.

(14) Khan, S.; Bijker, M. S.; Weterings, J. J.; Tanke, H. J.; Adema, G. J.; van Hall, T.; Drijfhout, J. W.; Melief, C. J. M.; Overkleeft, H. S.; van der Marel, G. A.; Filippov, D. V.; van der Burg, S. H.; Ossendorp, F. Distinct Uptake Mechanisms but Similar Intracellular Processing of Two Different Toll-like Receptor Ligand-Peptide Conjugates in Dendritic Cells. *J. Biol. Chem.* **2007**, *282*, 21145–21159.

(15) Gringhuis, S. I.; den Dunnen, J.; Litjens, M.; van der Vlist, M.; Geijtenbeek, T. B. H. Carbohydrate-Specific Signaling through the DC-SIGN Signalosome Tailors Immunity to Mycobacterium Tuberculosis, HIV-1 and Helicobacter Pylori. *Nat. Immunol.* **2009**, *10*, 1081–1088.

(16) Bertolotti, B.; Sutkeviciute, I.; Ambrosini, M.; Ribeiro-Viana, R.; Rojo, J.; Fieschi, F.; Dvořáková, H.; Kašáková, M.; Parkan, K.; Hlaváčková, M.; Nováková, K.; Moravcová, J. Polyvalent C-Glycomimetics Based on l -Fucose or d -Mannose as Potent DC-SIGN Antagonists. *Org. Biomol. Chem.* **2017**, *15*, 3995–4004.

(17) White, K. L.; Rades, T.; Furneaux, R. H.; Tyler, P. C.; Hook, S. Mannosylated Liposomes as Antigen Delivery Vehicles for Targeting to Dendritic Cells. *J. Pharm. Pharmacol.* **2006**, *58*, 729–737.

(18) Sangabathuni, S.; Vasudeva Murthy, R.; Chaudhary, P. M.; Surve, M.; Banerjee, A.; Kikkeri, R. Glyco-Gold Nanoparticle Shapes Enhance Carbohydrate-Protein Interactions in Mammalian Cells. *Nanoscale* **2016**, *8*, 12729–12735.

(19) Ahlén, G.; Strindelius, L.; Johansson, T.; Nilsson, A.; Chatzissavidou, N.; Sjöblom, M.; Rova, U.; Holgersson, J. Mannosylated Mucin-Type Immunoglobulin Fusion Proteins Enhance Antigen-Specific Antibody and T Lymphocyte Responses. *PLoS One* **2012**, *7*, e46959.

(20) Wilson, D. S.; Hirosue, S.; Raczy, M. M.; Bonilla-Ramirez, L.; Jeanbart, L.; Wang, R.; Kwissa, M.; Franetich, J.-F.; Broggi, M. A. S.; Diaceri, G.; Quaglia-Thermes, X.; Mazier, D.; Swartz, M. A.; Hubbell, J. A. Antigens Reversibly Conjugated to a Polymeric Glyco-Adjuvant Induce Protective Humoral and Cellular Immunity. *Nat. Mater.* **2019**, *18*, 175–185.

(21) Li, R.-J. E.; Hogervorst, T. P.; Achilli, S.; Bruijns, S. C.; Arnoldus, T.; Vivès, C.; Wong, C. C.; Thépaut, M.; Meeuwenoord, N. J.; van den Elst, H.; Overkleeft, H. S.; van der Marel, G. A.; Filippov, D. V.; van Vliet, S. J.; Fieschi, F.; Codée, J. D. C. C.; van Kooyk, Y. Systematic Dual

Targeting of Dendritic Cell C-Type Lectin Receptor DC-SIGN and TLR7 Using a Trifunctional Mannosylated Antigen. *Front. Chem.* **2019**, *7* . https://doi.org/10.3389/fchem.2019.00650.

(22) Tamburrini, A.; Colombo, C.; Bernardi, A. Design and Synthesis of Glycomimetics: Recent Advances. *Med. Res. Rev.* **2019**, No. April, 1–37.

(23) Zou, W. C-Glycosides and Aza-C-Glycosides as Potential Glycosidase and Glycosyltransferase Inhibitors. *Curr. Top. Med. Chem.* **2005**, *5*, 1363–1391.

(24) Girard, C.; Miramon, M.; de Solminihac, T.; Herscovici, J. Synthesis of 3-C-(6-O-Acetyl-2,3,4-Tri-O-Benzyl-α-d-Mannopyranosyl)-1-Propene: A Caveat. *Carbohydr. Res.* **2002**, *337*, 1769–1774.

(25) Jarikote, D. V.; O'Reilly, C.; Murphy, P. V. Ultrasound-Assisted Synthesis of C-Glycosides. *Tetrahedron Lett.* **2010**, *51*, 6776–6778.

(26) Touaibia, M.; Krammer, E.-M.; Shiao, T.; Yamakawa, N.; Wang, Q.; Glinschert, A.; Papadopoulos, A.; Mousavifar, L.; Maes, E.; Oscarson, S.; Vergoten, G.; Lensink, M.; Roy, R.; Bouckaert, J. Sites for Dynamic Protein-Carbohydrate Interactions of O- and C-Linked Mannosides on the E. Coli FimH Adhesin. *Molecules* **2017**, *22*, 1101.

(27) Sharma, P. K.; Kumar, S.; Kumar, P.; Nielsen, P. Selective Reduction of Mono- and Disubstituted Olefins by NaBH4 and Catalytic RuCl3. *Tetrahedron Lett.* **2007**, *48*, 8704–8708.

(28) Newlander, K. A.; Callahan, J. F.; Moore, M. L.; Tomaszek, T. A.; Huffman, W. F. A Novel Constrained Reduced-Amide Inhibitor of HIV-1 Protease Derived from the Sequential Incorporation of .Gamma.-Turn Mimetics into a Model Substrate. *J. Med. Chem.* **1993**, *36*, 2321–2331.

(29) Boger, D. L.; Yohannes, D.; Zhou, J.; Patane, M. A. Total Synthesis of Cycloisodityrosine, RA-VII, Deoxybouvardin, and N29-Desmethyl-RA-VII: Identification of the Pharmacophore and Reversal of the Subunit Functional Roles. *J. Am. Chem. Soc.* **1993**, *115*, 3420–3430.

(30) Jencks, W. P.; Gilchrist, M. Nonlinear Structure-Reactivity Correlations. The Reactivity of Nucleophilic Reagents toward Esters. *J. Am. Chem. Soc.* **1968**, *90*, 2622–2637.

(31) Raiber, E.-A.; Tulone, C.; Zhang, Y.; Martinez-Pomares, L.; Steed, E.; Sponaas, A. M.; Langhorne, J.; Noursadeghi, M.; Chain, B. M.; Tabor, A. B. Targeted Delivery of Antigen Processing Inhibitors to Antigen Presenting Cells via Mannose Receptors. *ACS Chem. Biol.* **2010**, *5*, 461–476.

(32) pHrodo Indicators for pH Determination - NL https://www.thermofisher.com/nl/en/home/brands/molecular-probes/key-molecular-probes-products/phrodo-indicators.html (accessed Sep 3, 2019).

(33) Hotta, C.; Fujimaki, H.; Yoshinari, M.; Nakazawa, M.; Minami, M. The Delivery of an Antigen from the Endocytic Compartment into the Cytosol for Cross-Presentation Is Restricted to Early Immature Dendritic Cells. *Immunology* **2006**, *117*, 97–107.

(34) Zhang, S.; Li, J.; Lykotrafitis, G.; Bao, G.; Suresh, S. Size-Dependent Endocytosis of Nanoparticles. *Adv. Mater.* **2009**, *21*, 419–424.

(35) Vennepureddy, A.; Thumallapally, N.; Motilal Nehru, V.; Atallah, J.-P.; Terjanian, T. Novel Drugs and Combination Therapies for the Treatment of Metastatic Melanoma. *J. Clin. Med. Res.* **2016**, *8*, 63–75.

(36) Chan, M.; Hayashi, T.; Kuy, C. S.; Gray, C. S.; Wu, C. C. N.; Corr, M.; Wrasidlo, W.; Cottam, H. B.; Carson, D. A. Synthesis and Immunological Characterization of Toll-Like Receptor 7 Agonistic Conjugates. *Bioconjug. Chem.* **2009**, *20*, 1194–1200.

(37) Wlodawer, A.; Miller, M.; Jaskolski, M.; Sathyanarayana, B.; Baldwin, E.; Weber, I.; Selk, L.; Clawson, L.; Schneider, J.; Kent, S. Conserved Folding in Retroviral Proteases: Crystal Structure of a Synthetic HIV-1 Protease. *Science (80-.).* **1989**, *245*, 616–621.

(38) Gential, G. P. P.; Hogervorst, T. P.; Tondini, E.; van de Graaff, M. J.; Overkleeft, H. S.; Codée, J. D. C.; van der Marel, G. A.; Ossendorp, F.; Filippov, D. V. Peptides Conjugated to 2-Alkoxy-8-Oxo-Adenine as Potential Synthetic Vaccines Triggering TLR7. *Bioorg. Med. Chem. Lett.* **2019**, *29*, 1340–1344.

(39) Chan, M.; Hayashi, T.; Kuy, C. S.; Gray, C. S.; Wu, C. C. N.; Corr, M.; Wrasidlo, W.; Cottam, H. B.; Carson, D. A. Synthesis and Immunological Characterization of Toll-Like Receptor 7 Agonistic Conjugates. *Bioconjug. Chem.* **2009**, *20*, 1194–1200.

(40) Matysiak, S.; Böldicke, T.; Tegge, W.; Frank, R. Evaluation of Monomethoxytrityl and Dimethoxytrityl as Orthogonal Amino Protecting Groups in Fmoc Solid Phase Peptide Synthesis. *Tetrahedron Lett.* **1998**, *39*, 1733–1734.

(41) Volbeda, A. G.; Kistemaker, H. A. V.; Overkleeft, H. S.; van der Marel, G. A.; Filippov, D. V.; Codée, J. D. C. Chemoselective Cleavage of *p* -Methoxybenzyl and 2-Naphthylmethyl Ethers Using a Catalytic Amount of HCl in Hexafluoro-2-Propanol. *J. Org. Chem.* **2015**, *80*, 8796–8806.

(42) Howard, K. T.; Chisholm, J. D. Preparation and Applications of 4-Methoxybenzyl Esters in Organic Synthesis. *Org. Prep. Proced. Int.* **2016**, *48*, 1–36.

(43) Geijtenbeek, T. B. H.; Gringhuis, S. I. C-Type Lectin Receptors in the Control of T Helper Cell Differentiation. *Nat. Rev. Immunol.* **2016**, *16*, 433–448.

(44) Brossart, P.; Zobywalski, A.; Grünebach, F.; Behnke, L.; Stuhler, G.; Reichardt, V. L.; Kanz, L.; Brugger, W. Tumor Necrosis Factor Alpha and CD40 Ligand Antagonize the Inhibitory Effects of Interleukin 10 on T-Cell Stimulatory Capacity of Dendritic Cells. *Cancer Res.* **2000**, *60*, 4485–4492.

(45) de Smedt, T.; van Mechelen, M.; De Becker, G.; Urbain, J.; Leo, O.; Moser, M. Effect of Interleukin-10 on Dendritic Cell Maturation and Function. *Eur. J. Immunol.* **1997**, *27*, 1229–1235.

(46) Corinti, S.; Albanesi, C.; la Sala, A.; Pastore, S.; Girolomoni, G. Regulatory Activity of Autocrine IL-10 on Dendritic Cell Functions. *J. Immunol.* **2001**, *166*, 4312–4318.

(47) Wieczorek, M.; Abualrous, E. T.; Sticht, J.; Álvaro-Benito, M.; Stolzenberg, S.; Noé, F.; Freund, C. Major Histocompatibility Complex (MHC) Class I and MHC Class II Proteins: Conformational Plasticity in Antigen Presentation. *Front. Immunol.* **2017**, *8*, 292.

(48) Engering, A.; Geijtenbeek, T. B. H.; van Vliet, S. J.; Wijers, M.; Liempt, E. van; Demaurex, N.; Lanzavecchia, A.; Fransen, J.; Figdor, C. G.; Piguet, V.; van Kooyk, Y. The Dendritic Cell-Specific Adhesion Receptor DC-SIGN Internalizes Antigen for Presentation to T Cells. *J. Immunol.* **2002**, *168*, 2118–2126.

(49) Schaft, N.; Willemsen, R. A.; de Vries, J.; Lankiewicz, B.; Essers, B. W. L.; Gratama, J.-W.; Figdor, C. G.; Bolhuis, R. L. H.; Debets, R.; Adema, G. J. Peptide Fine Specificity of Anti-Glycoprotein 100 CTL Is Preserved Following Transfer of Engineered TCR Genes Into Primary

632 Human T Lymphocytes. *J. Immunol.* **2003**, *170*, 2186–2194.

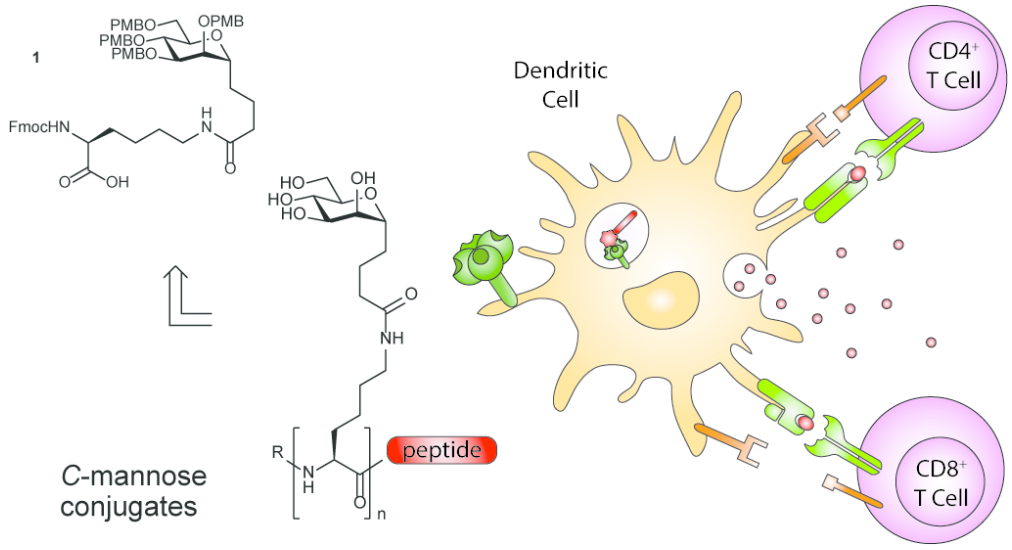

Graphical Abstract